AGU PUBLICATIONS

Geophysical Research Letters

RESEARCH LETTER
10.1002/2016GL070189

Special Section:
First results from NASA's Magnetospheric Multiscale (MMS) Mission

Key Points:
- Multispacecraft observations reveal an oxygen burst in the magnetosheath associated with a magnetotail particle injection event
- O^+ observed in the magnetosheath show finite-gyroradius effects consistent with entrainment on the magnetopause boundary
- H^+ observed in the magnetosheath are observed to be escaping due to a magnetic field component normal to magnetopause

Correspondence to:
J. H. Westlake,
joseph.westlake@jhuapl.edu

Citation:
Westlake, J. H., I. J. Cohen, B. H. Mauk, B. J. Anderson, D. G. Mitchell, M. Gkioulidou, B. M. Walsh, L. J. Lanzerotti, R. J. Strangeway, and C. T. Russell (2016), The permeability of the magnetopause to a multispecies substorm injection of energetic particles, *Geophys. Res. Lett.*, *43*, 9453–9460, doi:10.1002/2016GL070189.

Received 27 JUN 2016
Accepted 29 AUG 2016
Accepted article online 1 SEP 2016
Published online 28 SEP 2016

The permeability of the magnetopause to a multispecies substorm injection of energetic particles

J. H. Westlake[1], I. J. Cohen[1], B. H. Mauk[1], B. J. Anderson[1], D. G. Mitchell[1], M. Gkioulidou[1], B. M. Walsh[2], L. J. Lanzerotti[3,4], R. J. Strangeway[5], and C. T. Russell[5]

[1]Applied Physics Laboratory, The Johns Hopkins University, Laurel, Maryland, USA, [2]Department of Mechanical Engineering and Center for Space Physics, Boston University, Boston, Massachusetts, USA, [3]Bell Laboratories, Murray Hill, New Jersey, USA, [4]Center for Solar Terrestrial Research, New Jersey Institute of Technology, Newark, New Jersey, USA, [5]EPSS and IGPP, University of California, Los Angeles, California, USA

Abstract Leakage of ions from the magnetosphere into the magnetosheath remains an important topic in understanding the plasma physics of Earth's magnetopause and the interaction of the solar wind with the magnetosphere. Here using sophisticated instrumentation from two spacecraft (Radiation Belt Storm Probes Ion Composition Experiment on the Van Allen Probes and Energetic Ion Spectrometer on the Magnetospheric Multiscale) spaced uniquely near and outside the dayside magnetopause, we are able to determine the escape mechanisms for large gyroradii oxygen ions and much smaller gyroradii hydrogen and helium ions. The oxygen ions are entrained on the magnetosphere boundary, while the hydrogen and helium ions appear to escape along reconnected field lines. These results have important implications for not only Earth's magnetosphere but also other solar system magnetospheres.

1. Introduction

The magnetopause is the boundary that separates the shocked solar wind in the magnetosheath from the plasma in the magnetosphere, but it is permeable in that it allows particles and plasma from the magnetosphere to escape into the magnetosheath. In particular, energetic particles (greater than tens of keV) are often observed outside of the magnetopause boundary that is observed as more abrupt in lower energy particles and magnetic fields. The interaction of energetic particles with the Earth's magnetopause has been an active area of research [e.g., *Williams et al.*, 1979; *Krimigis et al.*, 1986; *Sibeck et al.*, 1987; *Mitchell et al.*, 1987; *Kudela et al.*, 1992], and it has been established that energetic particles escape the magnetosphere into the magnetosheath via a variety of processes: (1) acceleration at the dayside reconnection region and escape across a rotational discontinuity along reconnected magnetic field lines [*Speiser et al.*, 1981; *Cowley*, 1982]; (2) outward streaming along interconnected magnetosheath and magnetospheric magnetic field lines without acceleration [*Scholer et al.*, 1981]; (3) finite-gyroradius "leakage" as the particles cross a tangential discontinuity of the magnetopause [*Sibeck et al.*, 1987; *Sibeck and McEntire*, 1988; *Paschalidis et al.*, 1994]; or (4) escape into the magnetosheath caused by particle scattering in the magnetopause current sheet during enhanced solar wind dynamic pressure [*Zong and Wilken*, 1999].

Energetic oxygen bursts have been reported in the magnetosheath and upstream of the bow shock [*Zong and Wilken*, 1999; *Krimigis et al.*, 1986]. *Zong and Wilken* [1999] showed from Geotail data that these energetic oxygen bursts were of magnetospheric origin. However, it was unclear as to whether these ions are escaping into the magnetosheath or are moving along the magnetopause with their gyrocenters located inside the magnetosphere. The observations of *Zong and Wilken* [1999] also showed a lack of protons and helium leading to the conclusion that the oxygen ion bursts (1) originate from activity in the magnetosphere and not solar wind and (2) result from compression of the magnetopause that allows for previously trapped magnetospheric ions to be open to the magnetopause. The characteristics of the source populations and the injection dynamics inside the magnetosphere were not clear from these Geotail observations.

Questions remain concerning the degree to which energetic ions and electrons from the magnetosphere populate the magnetosheath and details of the processes responsible for their escape. It is particularly interesting in this regard to consider the dependence of transport on species since electrons, protons, and oxygen represent nearly 3 orders of magnitude in larmor radii for the same energy. In addition, constraining and confirming the role of internal magnetosphere dynamics in coordination with observations at the magnetopause is key to discriminating between candidate transport hypotheses. In this study, we present an event observed simultaneously by both the Magnetospheric Multiscale (MMS) within the magnetosheath and Van Allen Probes missions deep within the magnetosphere to examine the species dependence of energetic particle leakage.

2. Observations

We use data from MMS-Energetic Ion Spectrometer (EIS) [*Mauk et al.*, 2014] and Van Allen Probes Radiation Belt Storm Probes Ion Composition Experiment (RBSPICE) [*Mitchell et al.*, 2013], which are nearly identical energetic particle detectors based on a cylindrical time-of-flight geometry with six telescopes covering a 160° × 12° field of view (FOV) on the spinning spacecraft to sweep out a near full sky sample of look directions every spin. These instruments measure both the energy (E) of energetic ions and electrons and the time of flight (TOF) of ions. The E and TOF measurements allow separation of different species of energetic ions along distinct tracks in a TOF × E matrix which is separated into three data products in the instrument: protons, helium ions, and oxygen ions. The instrument does not distinguish between charge states of He or O. Because the magnetosphere was strongly compressed during the event described here, the MMS spacecraft was outside of its preprogrammed region of interest and most MMS instruments were either in a low-rate survey mode or not collecting measurements. EIS was in survey mode, which measures the three ion species and electrons with 1/8 spin (~2.5 s) resolution. The Van Allen Probes RBSPICE instrument was in its nominal operating mode and producing high rate measurements throughout this event. For this study we primarily focus on the MMS3 and Van Allen Probes B spacecraft; the spacing between the four MMS spacecraft was much smaller than the gyroradii of the energetic ions of interest here (in a 75 nT field the gyroradius of a 50 keV proton is 430 km and 13,000 km for a 150 keV O^+ ion), and no significant differences in the energetic particle behavior were observed between the spacecraft.

At 07:45 UT on 15 August 2015, the ACE spacecraft [*McComas et al.*, 1998; *Smith et al.*, 1998] observed an abrupt increase of the interplanetary magnetic field (IMF) magnitude and an increase in the solar wind dynamic pressure, along with several southward turnings of the IMF and an extended period of southward IMF that lasted until roughly 13:15 UT. The response of the magnetosphere resulting from the IMF southward turning and an increase in the dynamic pressure included a series of hot particle injection events in the magnetotail, identified from the energy-time dispersion signature of the ions. During this time the auroral electrojet (AE) index showed an abrupt rise to 1500 nT and the Dst index went from 10 nT to −22 nT (both retrieved from WDC for Geomagnetism, Kyoto) indicating an enhancement in the ring current. *Anderson et al.* [2016] show by comparison between the MMS data and Birkeland currents that the MMS magnetopause crossing occurred as the polar cap expanded and that the MMS foot point crossed through a region of strong convection associated with dusk flank reconnection. This evidence shows that the magnetopause was strongly eroded near dusk during this time.

RBSPICE first measured an energetic particle enhancement at 11:26 UT (Figures 1f–1h) in association, as described below, with the sudden compression of the magnetosphere. Subsequent injections, particularly evident with the oxygen data, are identified in the RBSPICE data as energy-dispersed features resulting from higher-energy particles that drift faster and arrive before the lower energies, the classic fingerprint of magnetically drifting particles after an energetic particle injection. While most evident in the oxygen data, the injection is also evident in proton and helium fluxes. The protons show less contrast than do the helium ions and the oxygen ions because the magnetosphere was already well populated with protons. A second injection event is then observed with RBSPICE at 13:05 UT (not shown). This enhancement also contains a train of injections that last until about 13:30 UT.

The four MMS spacecraft encountered a highly compressed magnetopause at 11:08 UT, identified by an increase in the magnitude and rotation of the magnetic field (Figure 1a), accompanied by a sharp boundary in the EIS observations (Figures 1b and 1c). The crossing appeared in EIS was as an abrupt reduction in intensities of protons and helium ions as the spacecraft moves from the magnetosphere to the magnetosheath. Across the boundary, the magnetic field increases in magnitude from about 50 nT to 100 nT and rotates from northward to southward.

MMS-EIS observed the first energetic particle enhancement in its oxygen channel at nearly the same time as RBSPICE (11:20 UT), followed by an energy-dispersed feature at 11:34 as additionally highlighted in the line

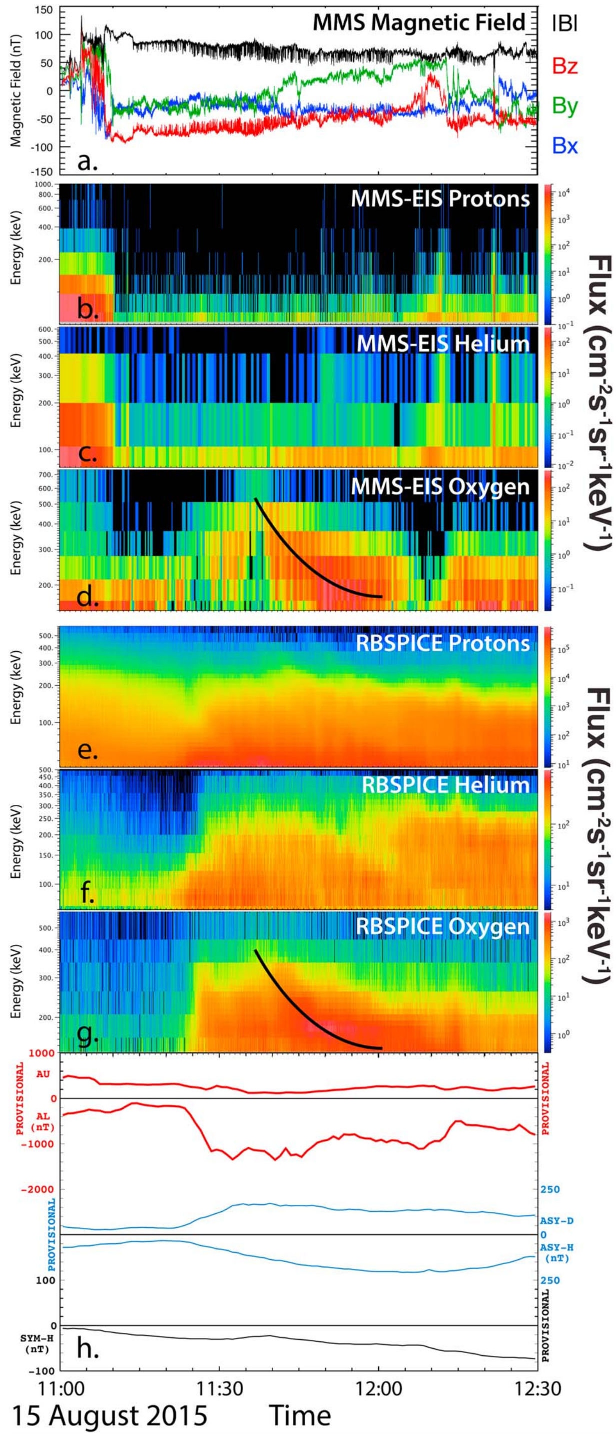

Figure 1. The time series of events on 15 August 2015 from 11:00 to 12:30 UTC as observed by MMS3 and Van Allen Probes B. Here we show the (a) MMS-Flux Gate Magnetometer (FGM) data [Russell et al., 2014], (b–d) energetic particle spectrograms for MMS-EIS, (e–g) Van Allen Probes RBSPICE spectrograms along with (h) various geomagnetic indices (retrieved from WDC for Geomagnetism, Kyoto). We also illustrate the energy dispersion observed by the MMS-EIS (Figure 1d) with a notional line that traces the general shape of the observations and is repeated over the RBSPICE observations (Figure 1g).

plots in Figure 2. We note that the spacing of the MMS and Van Allen Probes spacecraft was too small to see any differences in this feature between the different spacecraft within each mission. This energy-dispersed feature is interpreted here as an injection of energetic particles that then drift to the locations of the MMS and Van Allen Probes spacecraft with higher energies arriving before lower energies due to their faster drift times. Based on a rough guiding-center drift-time analysis, the energy-dispersed feature observed in oxygen ions at both MMS and Van Allen Probes is consistent with an energetic particle injection at 11:25 that has drifted to the location of the two spacecraft from the nightside. Although RBSPICE observed increases in helium and oxygen ion intensities in the 100 to 300 keV range of 1 to 2 orders of magnitude, EIS only observed the enhancement and injection at these energies in oxygen ions with no coincident increase in He. The particle enhancement initially observed by RBSPICE B at 11:25 is coincident with the drop in the *AL* index to −1200 nT. The initial enhancement shows little or no dispersion; we believe this is partially due to the compression of the magnetopause pushing preexisting dispersed ions inward. At the time, MMS was located within the magnetosheath, having crossed the magnetopause roughly 12 min prior [*Cohen et al.*, 2016; *Anderson et al.*, 2016]. Within the context of the gyrosounding interpretation given below, the magnetopause distance from the spacecraft is likely not greater than ~3000 km corresponding to the Larmor radius of a 150 keV O^+ in a 75 nT field.

Pitch angle distributions for selected representative energies of each species are shown in Figure 3 illustrating the dichotomy between the oxygen and protons: the oxygen ions are concentrated near 90° while the protons are monohemispherical, that is, confined primarily between 0° and 90° pitch angles. We attribute the proton directional behavior to boundary normal magnetic fields, an interpretation that is supported by the

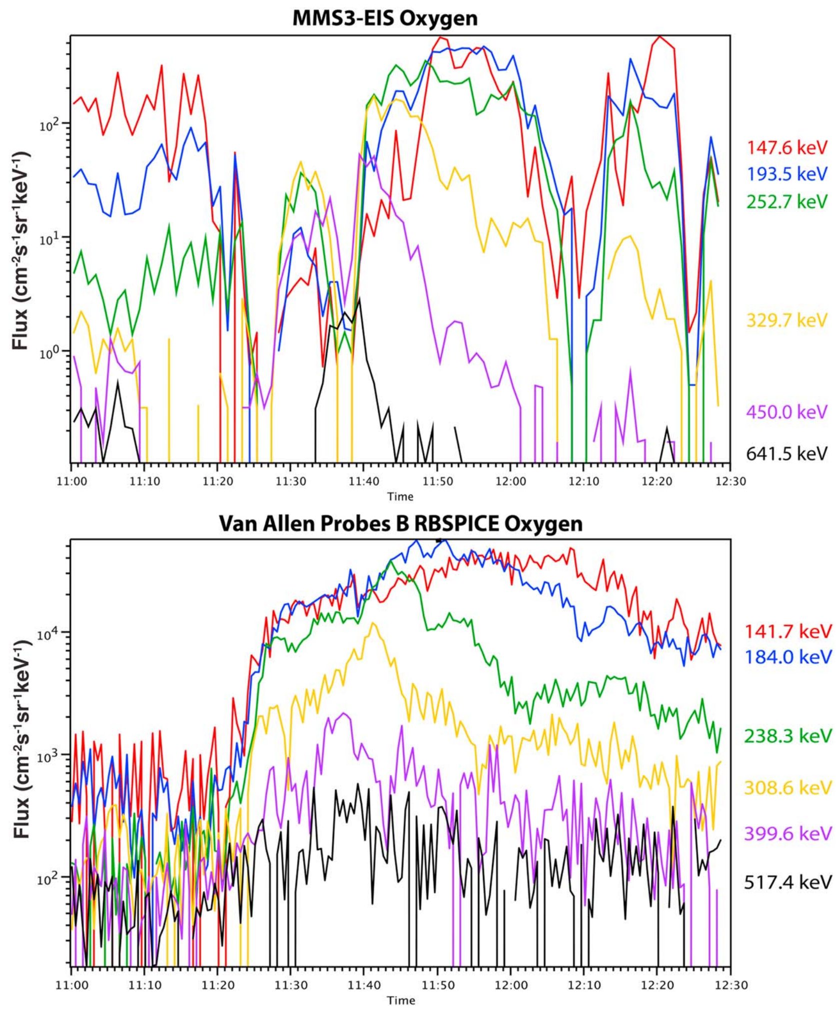

Figure 2. Oxygen ion fluxes from (top) MMS3 and (bottom) Van Allen Probes B with energies between 141 keV and 642 keV. The energy-dispersed feature is observed at both MMS and Van Allen Probes starting at 11:34 UT. The dispersion feature has nearly the same characteristics at both spacecraft in both the energies observed and timing.

detailed analysis of the electron and proton distributions at the magnetopause current layer [*Cohen et al.*, 2016]. The boundary normal magnetic field will allow for proton escape from the magnetosphere along the magnetic field direction. This conclusion raises the question of whether the oxygen observed with pitch angles centered at 90° is escaping the magnetosphere, which requires examining whether the oxygen is gyrotropic.

Full angular distributions of select MMS-EIS observed energetic ions are shown in Figure 4 plotted as azimuth angle versus elevation angle for six oxygen, one helium, and one proton energy channel. Prior to the magnetopause crossing, the oxygen ions are primarily observed in the lowest two energy channels with roughly isotropic distributions (not shown). After the magnetopause crossing the oxygen intensities narrow in both azimuth and elevation angle (show in the first column of Figure 4). These ions are observed with distributions centered near 90° pitch angles but are only observed from a limited range of azimuth angles. The azimuth direction corresponds to positive ions with gyrocenters Earthward of the spacecraft.

3. Discussion and Conclusions

We interpret the nongyrotropic signature in terms of oxygen ions with gyrotrajectories that maintain contact with the magnetosphere and that due to their large gyroradii (~3000 km or more) pass into the magnetosheath beyond the magnetopause current layer. This behavior is expected for a magnetospheric source. The 90° pitch angle particles are those that will reach the furthest from the magnetopause and the boundary

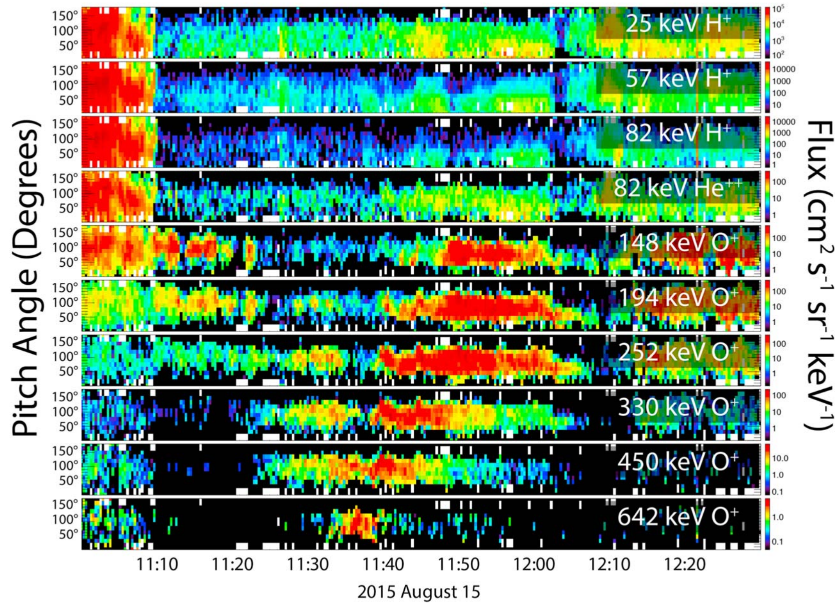

Figure 3. EIS instrument pitch angle distributions of energetic particles from 11:00 to 13:00 on 15 August 2015. These distributions show monodirectional protons (fluxes at 0° to 90° pitch angles) indicating escape across the magnetopause [*Cohen et al.*, 2016] that are observed during the same time interval when apparently trapped (peaking near 90° pitch angle) distributions of oxygen and helium are observed that are consistent with entrainment on the magnetopause boundary in Speiser orbits.

geometry will limit the observable azimuthal distribution as observed. As expected from this hypothesis, the location in azimuth of the peak in the oxygen responses is roughly −45°, which is the expected direction for ions with velocity vectors that are roughly tangent to the nominal magnetopause surface at the local time where the event was observed and consistent with the southward orientation of the magnetosheath magnetic field. The oxygen data are therefore not consistent with field-aligned escape due to its pitch angle distribution, which would be centered along the field-aligned direction if field-aligned escape was occurring. The oxygen could be consistent with either finite-gyroradius leakage or scattering of particles in the interaction with the magnetopause.

The protons show a very different behavior during this time. The proton enhancements, especially from 11:42–11:59 UT, are confined to pitch angles less than 90°. Both monohemispherical streaming electrons and protons were observed during this magnetopause crossing [*Cohen et al.*, 2016]. We interpret the protons observed as streaming along open field lines or scattered into the magnetopause due to their pitch angle distribution, which is centered on the field-aligned direction. We do not observe acceleration as the particles flow along the magnetic field. At the same time, the helium observations show both field-aligned components and 90° pitch angle features. Because MMS was in survey mode, the number of energy bins is reduced and hence the energy bin width is large (60 keV–110 keV) and spans a large range of gyroradii (~425 km to ~850 km). This bin appears to contain both smaller gyroradius particles that will behave like the protons and stream along the magnetic field and larger gyroradius particles that behave like the oxygen and reach out from the magnetosphere into the magnetosheath. We attribute the proton escape to a magnetic field component that is normal to the magnetopause. This normal component appears to be directly affecting the proton escape from the magnetosphere and does not appear to be affecting the oxygen ions at the boundary. This behavior is confirmed by the modeling of *Mauk et al.* [2016], and the differences result from the order of magnitude differences in the oxygen and proton gyroradii.

Escape along newly reconnected field lines does not appear to be responsible for the oxygen and higher-energy helium observations. The oxygen and helium both have distributions with significant components at 90° pitch angles and limited azimuthal distributions indicating that these particles are reaching out from the magnetosphere into the magnetosheath and not escaping along newly reconnected field lines. The large gyroradius of these particles allow them to reach out into the magnetosheath, and therefore either finite-gyroradius

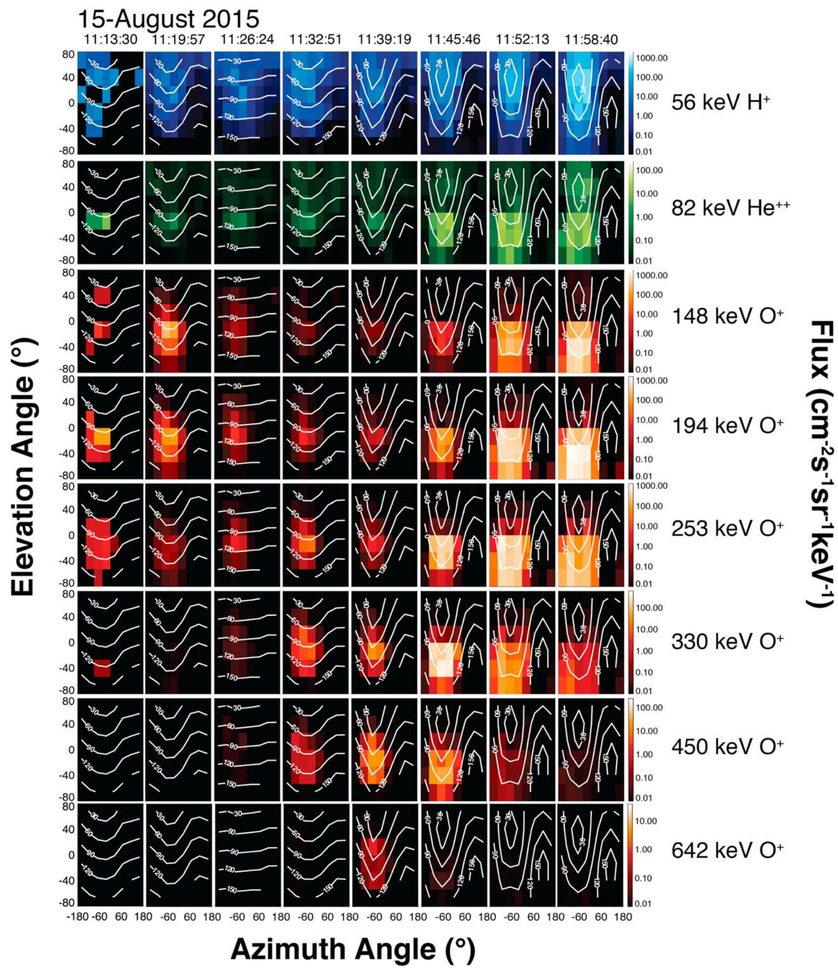

Figure 4. A time series from 11:13 to 11:58 of the MMS-EIS observations of energetic H^+ (blues), He^{++} (greens), and O^+ (reds) intensities plotted as elevation angle versus azimuth angle with pitch angle contours are plotted over the particle intensities. The figure is organized with energy increasing by row with the highest energies in the bottom row of plots and the lowest energies in the top row, and each row is labeled with the center energy of the bin.

leakage or scattering in the interaction with the magnetopause could be consistent with the pitch angle distributions. *Mauk et al.* [2016] showed that the detailed structure of the boundary played a crucial role in whether particles were entrained on the boundary or were scattered onto escaping trajectories. The simulated trajectories from this model are reproduced in Figure 5 and show that low-energy protons with 90° pitch angles could be scattered into the magnetosheath, while energetic oxygen would be entrained onto the boundary. Furthermore, scattering in the boundary tends to shift protons to more field-aligned directions [*Mauk et al.*, 2016]. Therefore, these protons could have been scattered in their interaction with the boundary or could be escaping along newly reconnected field lines. We therefore interpret the oxygen and the higher-energy helium ions to be entrained on the magnetopause boundary and only observed in the magnetosheath due to their large gyroradii, while the protons could either be escaping along newly reconnected field lines or being scattered into the magnetosheath due to the interaction with the boundary.

Figure 5 schematically shows our interpretation of the signatures of oxygen ions and protons and shows results from a kinetic model of the interactions of energetic particles with magnetopause structures documented by *Mauk et al.* [2016]. The model emulates the measured configuration of the fields (electric and magnetic) in the magnetosphere and magnetosheath and the rotational structure of the magnetic field within the 400 km thick model magnetopause used here [cf. *Cohen et al.*, 2016] and explicitly solves the particle trajectories. For this run, the magnetopause contains a boundary normal magnetic field that is 5% of the nominal magnetosheath magnetic field strength. In the model, protons (and electrons) indeed do cross the

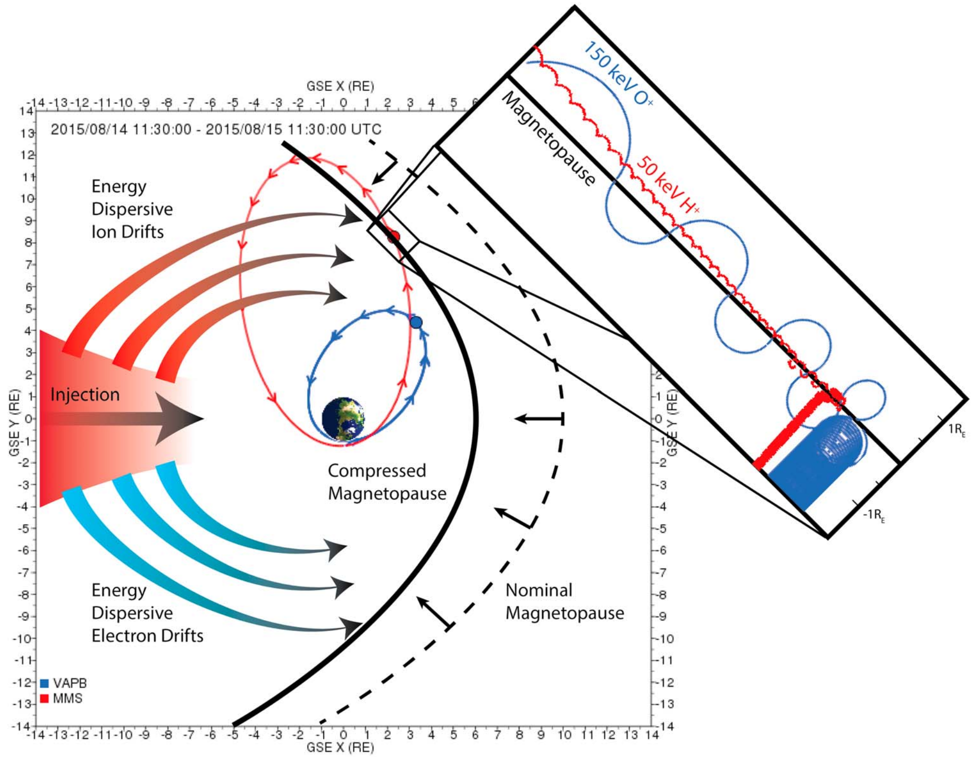

Figure 5. The location of the Van Allen Probes spacecraft and MMS spacecraft at 11:30 UTC on 15 August 2015. This figure also shows a notional magnetopause location displaced Earthward relative to its average location and a schematic of the energetic particle injection observed by these spacecraft. The figure inset shows 50 keV H^+ and 150 keV O^+ trajectories at the magnetopause from the model of *Mauk et al*. [2016].

boundary, giving rise to magnetic field-aligned streaming particles (the red trace in the inserted figure). Oxygen ions (blue trace), with their much larger gyroradii, behave much differently and execute Speiser orbits which entrained them in a streaming population parallel to and in the vicinity of the boundary. The simultaneous observation of disparate pitch angle distributions and streaming for oxygen and protons reported here is consistent with the model.

In summary, we have presented a multispacecraft observation of an oxygen-rich energetic particle injection event inside of the magnetosphere by the Van Allen Probes spacecraft and also just outside the magnetopause in Earth's magnetosheath by the MMS mission. This event was used as a test case to probe aspects of the permeability of the magnetopause to energetic particles. This observation of energetic oxygen bursts adds to the previously observed cases at Earth and several other solar system bodies [e.g., *Baker et al*., 1984; *Krimigis et al*., 1985; *Sergis et al*., 2013], adding detail into the processes responsible for particle escape from the magnetosphere. We have considered the following mechanisms for particle escape from the magnetosphere: escape along newly reconnected field lines, finite-gyroradius leakage, and scattering in the interaction with the magnetopause finding that the protons and low-energy helium were escaping along newly reconnected field lines and that the higher-energy helium and oxygen ions were exhibiting finite-gyroradius leakage.

Our observations uniquely reveal the behaviors of energetic oxygen and protons, with the oxygen ions appearing to be entrained on the boundary while the protons appear to be escaping along reconnected field lines. Contrary to interpretations of some previous reported events [e.g., *Zong et al*., 2001], the oxygen ions that we measure, with their large gyroradii, do not appear to be participating in field-aligned escape from the magnetosphere at the same time than are other ions with substantially smaller gyroradii. *Zong et al*. [2001] attributed a similar event as oxygen escaping into the magnetosheath along newly reconnected field lines. The basis of this conclusion is a principle axis analysis of the magnetic field to determine whether it is open or closed at the time, not on the actual behavior of the particles, which in this case were very similar to the oxygen shown in this paper (centered on 90° pitch angles with a flow away from the magnetopause).

Zong and Wilken [1999] also show a multispacecraft observation of an energetic particle injection associated with enhanced oxygen outside of the magnetopause. This observation reported energetic electron enhancements in the magnetosphere associated with an energetic particle injection but did not have coincident observations of energetic oxygen in the magnetosphere. These similar observations were also devoid of protons and were unable to witness the field-aligned proton streaming.

Acknowledgments
This work was supported by the Magnetospheric Multiscale (MMS) mission of NASA's Science Directorate Heliophysics Division via subcontract to the Southwest Research Institute. The dedication and expertise of the MMS development and operations teams are greatly appreciated. Work at JHU/APL, UCLA, UNH, and SwRI was supported by NASA contract NNG04EB99C. The RBSPICE instrument was supported by JHU/APL subcontract 937836 to the New Jersey Institute of Technology under NASA Prime contract NAS5-01072. As of 1 March 2016, MMS data are available for 1 September 2015 through 31 January 2016 from the MMS Science Data Center web site: https://lasp.colorado.edu/mms/sdc/. Data for 15 August 2015 are available upon request. The RBSPICE data are publically available from rbspice.ftecs.com

References

Anderson, B. J., et al. (2016), Electrodynamics context of magnetopause dynamics observed by magnetospheric multiscale, *Geophys. Res. Lett.*, *43*, 5988–5996, doi:10.1002/2016GL069577.

Baker, D. N., R. D. Zwickl, S. M. Krimigis, J. F. Carbary, and M. H. Acuña (1984), Energetic particle transport in the upstream region of Jupiter: Voyager results, *J. Geophys. Res.*, *89*(A6), 3775–3787, doi:10.1029/JA089iA06p03775.

Cohen, I. J., et al. (2016), Observations of energetic particles at the magnetopause: Early results from the MMS Energetic Ion Spectrometer (EIS), *43*, 5960–5968, doi:10.1002/2016GL068689.

Cowley, S. W. H. (1982), The causes of convection in the Earth's magnetosphere: A review of developments during the IMS, *Rev. Geophys.*, *20*(3), 531–65, doi:10.1029/RG020i003p00531.

Krimigis, S. M., R. D. Zwickl, and D. N. Baker (1985), Energetic ions upstream of Jupiter's bow shock, *J. Geophys. Res.*, *90*(A5), 3947–3960, doi:10.1029/JA090iA05p03947.

Krimigis, S. M., D. G. Sibeck, and R. W. McEntire (1986), Magnetospheric particle injection and the upstream ion event of September 5, 1984, *Geophys. Res. Lett.*, *13*(13), 1376–1379, doi:10.1029/GL013i013p01376.

Kudela, K., D. G. Sibeck, M. Slivka, S. Fischer, V. N. Lutsenko, and D. Venkatesan (1992), Energetic electrons and ions in the magnetosheath at low and medium latitudes: Prognoz 10 data, *J. Geophys. Res.*, *97*(A10), 14,849–14,857, doi:10.1029/92JA01134.

Mauk, B. H., et al. (2014), The Energetic Particle Detector (EPD) investigation and the Energetic Ion Spectrometer (EIS) for the Magnetospheric Multiscale (MMS) mission, *Space Sci. Rev.*, *199*(1), 471–514, doi:10.1007/s11214-014-0055-5.

Mauk, B. H., I. J. Cohen, J. H. Westlake, and B. J. Anderson (2016), Modeling magnetospheric energetic particle escape across Earth's magnetopause as observed by the MMS mission, *Geophys. Res. Lett.*, *42*, 4081–4088, doi:10.1002/2016GL068856.

McComas, D. J., S. J. Bame, P. Barker, W. C. Feldman, J. L. Phillips, P. Riley, and J. W. Griffee (1998), Solar Wind Electron Proton Alpha Monitor (SWEPAM) for the Advanced Composition Explorer, *Space Sci. Rev.*, *86*, 563–612.

Mitchell, D. G., F. Kutchko, D. J. Williams, T. E. Eastman, L. A. Frank, and C. T. Russell (1987), An extended study of the low-latitude boundary layer on the dawn and dusk flanks of the magnetosphere, *J. Geophys. Res.*, *92*(A7), 7394–7404, doi:10.1029/JA092iA07p07394.

Mitchell, D. G., et al. (2013), Radiation Belt Storm Probes Ion Composition Experiment (RBSPICE), *Space Sci. Rev.*, *179*(1–4), 263–308, doi:10.1007/s11214-013-9965-x.

Paschalidis, N. P., E. T. Sarris, S. M. Krimigis, R. W. McEntire, M. D. Levine, I. A. Daglis, and G. C. Anagnostopoulos (1994), Energetic ion distributions on both sides of the Earth's magnetopause, *J. Geophys. Res.*, *99*(A5), 8687–8703, doi:10.1029/93JA03563.

Russell, C. T., et al. (2014), The magnetospheric multiscale magnetometers, *Space Sci. Rev.*, *199*(1-4), 189–256.

Scholer, M., D. Hovestadt, F. M. Ipavich, and G. Gloeckler (1981), Upstream energetic ions and electrons: Bow shock-associated or magnetospheric origin? *J. Geophys. Res.*, *86*(A11), 9040–9046, doi:10.1029/JA086iA11p09040.

Sergis, N., C. M. Jackman, A. Masters, S. M. Krimigis, M. F. Thomsen, D. C. Hamilton, D. G. Mitchell, M. K. Dougherty, and A. J. Coates (2013), Particle and magnetic field properties of the Saturnian magnetosheath: Presence and upstream escape of hot magnetospheric plasma, *J. Geophys. Res. Space Physics*, *118*, 1620–1634, doi:10.1002/jgra.50164.

Sibeck, D. G., and R. W. McEntire (1988), Multiple satellite observations of leakage of particles from the magnetosphere, *Adv. Space Res.*, *8*(9–10), 201–216, doi:10.1016/0273-1177(88)90133-0.

Sibeck, D. G., R. W. McEntire, A. T. Y. Lui, R. E. Lopez, S. M. Krimigis, R. B. Decker, L. J. Zanetti, and T. A. Potemra (1987), Energetic magnetospheric ions at the dayside magnetopause: Leakage or merging? *J. Geophys. Res.*, *92*(A11), 12,097–114, doi:10.1029/JA092iA11p12097.

Smith, C. W., J. L'Heureux, N. F. Ness, M. H. Acuña, L. F. Burlaga, and J. Scheifele (1998), The ACE magnetic fields experiment, *Space Sci. Rev.*, *86*, 613–632.

Speiser, T. W., D. J. Williams, and H. A. Garcia (1981), Magnetospherically trapped ions as a source of magnetosheath energetic ions, *J. Geophys. Res.*, *86*(A2), 723–32, doi:10.1029/JA086iA02p00723.

Williams, D., T. Fritz, B. Wilken, and E. Keppler (1979), An energetic particle perspective of the magnetopause, *J. Geophys. Res.*, *84*(A11), 6385–6396, doi:10.1029/JA084iA11p06385.

Zong, Q.-G., and B. Wilken (1999), Bursty energetic oxygen events in the dayside magnetosheath: GEOTAIL observations, *Geophys. Res. Lett.*, *26*(22), 3349–52, doi:10.1029/1999GL003634.

Zong, Q.-G., B. Wilken, S. Y. Fu, T. A. Fritz, A. Korth, N. Hasebe, D. J. Williams, and Z.-Y. Pu (2001), Ring current oxygen ions escaping into the magnetosheath, *J. Geophys. Res.*, *106*(A11), 25,541–25,556, doi:10.1029/2000JA000127.